

UNCLASSIFIED

AD NUMBER

AD842809

LIMITATION CHANGES

TO:

Approved for public release; distribution is unlimited.

FROM:

Distribution authorized to U.S. Gov't. agencies and their contractors; Critical Technology; SEP 1968. Other requests shall be referred to Air Force Flight Dynamics Lab., Wright-Patterson AFB, OH 45433.

AUTHORITY

AFFDL ltr, 12 Mar 1973

THIS PAGE IS UNCLASSIFIED

AFFDL-TR-68-100

AD0842809

20090520 205

STUDY OF FATIGUE CRACK INITIATION FROM FLAWS USING FRACTURE MECHANICS THEORY

R. G. FORMAN

TECHNICAL REPORT AFFDL-TR-68-100

SEPTEMBER 1968

This document is subject to special export controls and each transmittal to foreign governments or foreign nationals may be made only with prior approval of the Air Force Flight Dynamics Laboratory (FDTR), Wright-Patterson AFB, Ohio 45433.

NOTICES

When Government drawings, specifications, or other data are used for any purpose other than in connection with a definitely related Government procurement operation, the United States Government thereby incurs no responsibility nor any obligation whatsoever; and the fact that the Government may have formulated, furnished, or in any way supplied the said drawings, specifications, or other data, is not to be regarded by implication or otherwise as in any manner licensing the holder or any other person or corporation, or conveying any rights or permission to manufacture, use, or sell any patented invention that may in any way be related thereto.

This document is subject to special export controls and each transmittal to foreign governments or foreign nationals may be made only with prior approval of the Air Force Flight Dynamics Laboratory, Wright-Patterson AFB, Ohio 45433.

The distribution of this report is limited because unlimited distribution would significantly diminish the technological lead time of the United States and friendly foreign nations by revealing techniques having a potential strategic or economic value not generally known throughout the world.

Copies of this report should not be returned unless return is required by security considerations, contractual obligations, or notice on a specific document.

**STUDY OF FATIGUE CRACK INITIATION
FROM FLAWS USING FRACTURE
MECHANICS THEORY**

R. G. FORMAN

This document is subject to special export controls and each transmittal to foreign governments or foreign nationals may be made only with prior approval of the Air Force Flight Dynamics Laboratory (FDTR), Wright-Patterson AFB, Ohio 45433.

FOREWORD

This report describes an experimental and theoretical study on the fatigue crack initiation from flaws in cyclic loaded structures. The experimental work was conducted from July 1966 to August 1967, by the Structures Test Branch, Structures Division, Air Force Flight Dynamics Laboratory. The test engineer for the program was Mr. R. L. Schneider. Mr. H. E. Andrews, test technician, prepared the specimens, conducted the tests, and recorded the data.

This report and the initial test program plan was written by Mr. R. G. Forman, Aerospace Engineer, Theoretical Mechanics Branch, Structures Division, Air Force Flight Dynamics Laboratory, under Project No. 1467, "Structural Analysis Methods," Task 146704, "Structural Fatigue Analysis," with Mr. Robert M. Bader acting as Project Engineer.

The manuscript was released by the author in May 1968 for publication as a technical report.

This technical report has been reviewed and is approved.

A handwritten signature in black ink, appearing to read "Francis J. Janik". The signature is stylized with a large initial "F" and a long horizontal stroke.

FRANCIS J. JANIK
Chief, Theoretical Mechanics Branch
Structures Division
Air Force Flight Dynamics Laboratory

ABSTRACT

This report presents theoretical and experimental results on fatigue crack initiation from flaws in cyclic loaded structures. The results indicated that the fracture mechanics stress-intensity-factor range, ΔK , is the governing parameter for inducing fatigue crack initiation from a flaw. Theoretical crack growth analysis indicated that when initiating an "engineering size" fatigue crack from a flaw, most of the cyclic behavior was crack growth and only a small part was nucleation.

This abstract is subject to special export controls and each transmittal to foreign governments or foreign nationals may be made only with prior approval of the Air Force Flight Dynamics Laboratory (FDTR), Wright-Patterson AFB, Ohio.

TABLE OF CONTENTS

| SECTION | PAGE |
|------------------------|------|
| I INTRODUCTION | 1 |
| II SUMMARY | 2 |
| III TECHNICAL APPROACH | 3 |
| IV TEST PROGRAM | 5 |
| V TEST RESULTS | 6 |
| REFERENCES | 10 |
| APPENDIX | 13 |

ILLUSTRATIONS

| FIGURE | | PAGE |
|--------|--|------|
| 1. | Variation in ΔK with N_i for Flaws in Butt-Welded 3/4-Inch-Thick HY-80 Steel Strips | 15 |
| 2. | Variation in Yield-Zone Size with Notch Tip Radius | 16 |
| 3. | Variation of Apparent Fracture Toughness with Root Radius for Centrally Notched 7075-T6 Aluminum Plates | 17 |
| 4. | Comparison of Theoretical Crack Growth of .010-Inch with First Observation of .010-Inch Fatigue Cracks in Notched Sheets of 7075-T6 Aluminum | 18 |
| 5. | Comparison of Theoretical Crack Growth of .0025-Inch with First Observation of .0025-Inch Fatigue Cracks in Notched Sheets of 2014-T6 Aluminum | 19 |
| 6. | Comparison of Applied Cyclic Stress Range with Cycles to Fatigue Crack Initiation from Blunt Flaws in 7075-T6 Aluminum Plates | 20 |
| 7. | Geometry of Plastic Zone Boundaries at the Tip of Sharp and Blunt Elliptic Notches in a Plate Subjected to Uniaxial Tension | 21 |

TABLES

| TABLE | | |
|-------|--|----|
| I. | Test Data for Initiation of 0.010-Inch Cracks in 0.050-Inch-Thick 7075-T6 Aluminum Sheet Specimens Fatigue Cycled at $R = 0$ | 22 |
| II. | Theoretical Values of Plastic Zone Size | 23 |

SYMBOLS

| | |
|-----------------------------------|---|
| C, n | Material constants for crack propagation |
| $F()$ | A function |
| K | Fracture mechanics stress-intensity factor |
| ΔK | Stress-intensity-factor range (maximum K - minimum K in a load cycle) |
| K_a | Apparent fracture toughness for blunt crack |
| K_C | Critical stress-intensity factor for fracture |
| N | Load cycles |
| N_i | Number of load cycles for fatigue crack initiation |
| R | Radius of hole, minimum K /maximum K in a load cycle |
| Y | Material tensile yield stress |
| a | Flaw length (half length for central slit), radius of penny-shaped flaw |
| x, y, z | Cartesian coordinates |
| r, θ | Polar coordinates |
| r_p | Dimension of yield, or plastic, zone at $\theta = 0$ for finite root radius flaws |
| t | Thickness of sheet |
| w | Theoretical yield-zone width for $\rho = 0$ flaws |
| w_c | Theoretical critical yield-zone width for $\rho = 0$ flaws |
| σ_0 | Applied stress on sheet |
| $\Delta\sigma_0$ | Applied stress range in a load cycle (maximum σ_0 - minimum σ_0) |
| $\sigma_x, \sigma_y, \sigma_z$ | Normal and shear stresses |
| $\tau_{xy}, \tau_{xz}, \tau_{yz}$ | |
| σ_0 | Tangential stress |
| $\Delta\sigma_t$ | Tangential stress range in a load cycle |
| β | Angular position of notch on hole boundary |
| ρ | Radius of curvature at crack tip |
| ν | Poisson's ratio |

SECTION I

INTRODUCTION

Data exists which indicates that fatigue cracks in cyclic loaded structures often originate from flaws. The flaws originate either during manufacture of the structure in the form of tool marks and weld flaws, or during usage of the structure, as nicks or scratches. The current practice in estimating the fatigue life of a flawed structure is to conduct crack propagation analysis and to assume that crack growth begins with the first load cycle. Recently improved theories exist for crack growth behavior (e.g., see References 1 and 2), and when environmental effects are taken into account, the remaining life of fatigue-cracked structures can usually be predicted.

The basic difficulty in using crack propagation analysis alone, however, is that all flaws are arbitrarily assumed to be so sharp or large that the crack initiation phase can be neglected. The analysis is questionable, for example, for very fine surface scratches in aluminum structures where experience has shown that these scratches do not have a measurable effect on the fatigue life. Very little is known about the effect of flaw size and flaw tip radius on fatigue initiation, and this problem needs to be resolved before the cyclic behavior of real structures can be adequately understood.

The purpose of the study in this report, then, was to investigate the initiation phase of fatigue cracks which originate from flaws. The study was essentially an experimental effort using centrally notched sheets of 7075-T6 aluminum alloy with various flaw geometries, sizes, and root radii. The experimental results were analyzed using the stress-intensity-factor concept from fracture mechanics theory. Corrections were made to account for the finite root radii of the flaw tips.

SECTION II

SUMMARY

A theoretical and experimental study has shown that the fracture mechanics stress-intensity-factor approach is applicable to the analysis of fatigue crack initiation from flaws. The relative stress-intensity-factor range, $\Delta K/K_a$, appeared to be the governing parameter for causing initiation of an "engineering size" fatigue crack from a flaw in a cyclic loaded structure. Initiation of an "engineering size" crack was difficult to define, however, and theoretical analysis of the data indicated that a large percentage of the cyclic behavior (i.e., 90%) was probably crack propagation from an unknown micro-size to an "engineering size" crack and very little was nucleation. Finally, a limiting size of flaw was determined which would not have a measurable effect on the fatigue life of structures manufactured from 7075-T6 aluminum alloy.

SECTION III

TECHNICAL APPROACH

Currently, general agreement exists with the Paris theory (Reference 3), which states that the stress-intensity-factor range, ΔK , may be viewed as the driving force for fatigue crack propagation. Since crack growth rate is governed by ΔK , it is reasonable to assume that the number of cycles required to initiate a fatigue crack from a sharp notch or flaw is also determined by ΔK . Limited data exists which shows that this is indeed true. Figure 1, for example, shows experimental results for crack initiation from flaws in butt-welded HY-80 steel strips. Use of the stress-intensity factor for a penny-shaped internal flaw appears to give very consistent results in the data for cycles to crack initiation.

One problem in either an experimental or theoretical study of fatigue crack initiation is the proper definition of crack initiation. Usually, there exists a micro-crack growth phase and a macro-crack growth phase in fatigue (e.g., see the related study of Schijve, Reference 4), and the initiation of an "engineering size" could be considered as the crack size when the macro-crack growth phase commences. This could be a crack length of .002 to .003 inch, which is about the minimum size that can be clearly distinguished under an optical microscope, or it can be a length of .010 inch, which is approximately the minimum length that can be distinguished with the naked eye. For the present study, both definitions were used, and the results indicated that the technical approach was applicable for both lengths.

In crack propagation analysis, a valid approach in describing either the crack growth rate or the cycles to failure is to assume that the behavior is a function of the relative stress-intensity-factor range, $\Delta K/K_c$. The validity of this approach was confirmed in the current study for determining crack initiation behavior. One difference, though, is that K_c , or apparent K_c , is not a constant but depends upon the root radius of the notch tip. A new ratio, $\Delta K/K_a$, was defined to account for the variation where K_a is the apparent fracture toughness which is corrected for the finite root radius.

The correction factor used to correct K_c for the effect of the finite root radius was derived from a theoretical analysis of the yield zone at the tip of a blunt crack. The analysis is described in the Appendix, but the results of the analysis is that a functional relationship exists between the yield-zone size and the crack tip root radius. The relationship is shown graphically in Figure 2 for the cases of both plane stress and plane strain.

A series of tests were conducted on centrally notched sheets of 7075-T6 aluminum alloy to measure the effect of crack root radius on K_c . The results are shown in Figure 3 and listed in Table I where $\beta = 90^\circ$ and $N_i = 1$. The results indicate that the apparent fracture toughness can be determined from the following formula:

$$K_a = \left(\frac{r_p}{w_c} \right) K_c \quad (1)$$

where (r_p/w_c) is the relative size of the yield zone, as shown in Figure 2.

In Figure 3 is shown an experimental curve for the data of Mulherin, Armiento, and Markus (Reference 5) for 60-degree v-shaped edge-notched specimens. Their data indicates a much greater increase in apparent fracture toughness with root radius than the centrally notched specimen data exhibits. The discrepancy is difficult to evaluate because neither notch geometry has a true solution for the stress distribution. For instance, the central notch geometry is analyzed by assuming a flattened elliptical hole in a plate. For the edge notch we assume a hyperbolic notch geometry. No solutions exist for either the case of an edge notch with straight edges for which the root radius is independent of the flank angle or for the central slit with variable root radii. For the present study, the central notch configuration was assumed to give the most accurate representation of apparent fracture toughness, and this configuration was used for the basis of Equation 1.

SECTION IV

TEST PROGRAM

All tests were conducted on .050-inch-thick sheets of bare 7075-T6 aluminum alloy. The size and geometry of the specimens are shown in Figure 4. The grain direction of the material was in the lengthwise direction of the specimen, or parallel to the direction of load.

The specimens were all tested in the same hydraulic loading machine for both the static and fatigue tests. The cyclic loading was a sinusoidal type of loading with frequencies between one and four cycles per second.

Fatigue crack initiation was determined by visual observation using a forty power stereomicroscope. The specimen surfaces were polished in the area of the notch tips to assist in distinguishing the smallest visible fatigue crack. After fatigue crack initiation was obtained, the crack size was measured with a forty power toolmaker's microscope. The sizes varied between .005 and .015 inch in length, and, thus, crack initiation was defined as the cycle at which an approximate .010-inch-long crack was first observed.

The smallest flaw tip radius for any specimen was .001 inch. This would probably be close to the minimum tip radius for an actual flaw in a structure because the radius was obtained by sawing with a razor blade. The sharpest razor-blade-cut flaws (.001 and .002 inch tip radius) were made with a special sawing machine made for the test program. The .004-inch-radius flaws were made by sawing manually. Flaws, .007-inch and larger, were obtained by drilling holes and cutting slots to the holes. The radii were checked with the toolmaker's microscope and the tolerance was found to be approximately $\pm .001$ inch for the drilled holes and $\pm .0005$ inch for the razor-blade cuts. These tolerances, or accuracies, should be applied to all listed values for the tip radii in Table I.

Both mechanical methods, such as drilling, and electrical discharge methods (EDM) were attempted to determine the best procedure for introducing the

notches in the specimens. The EDM method gave a significantly more accurate and better notch root, but the mechanical method was used because flaws introduced by this method would be more typical of actual flaws, such as tool marks or scratches.

SECTION V

TEST RESULTS

The test results for the notched 7075-T6 sheet specimens are shown in Figure 4, and the detail data is listed in Table I. The data is essentially for three types of notch geometry. Each geometry was analyzed using a different formula for the stress-intensity factor. The formula for each geometry was obtained from Reference 6 and they are given as follows:

- (1) Central slit ($R = 0$, $\beta = 90^\circ$):

$$\Delta K = \Delta \sigma_0 \sqrt{\pi a} \quad (2)$$

- (2) Notched circular hole with $\beta = 90^\circ$:

$$\Delta K = \Delta \sigma_0 \sqrt{\pi a} \left[F\left(\frac{a}{R}\right) \right] \quad (3)$$

where $F\left(\frac{a}{R}\right)$ is tabulated as follows:

| a/R | $F\left(\frac{a}{R}\right)$ |
|-------|-----------------------------|
| 0.00 | 3.39 |
| 0.10 | 2.73 |
| 0.20 | 2.41 |
| 0.30 | 2.15 |
| 0.40 | 1.96 |
| 0.50 | 1.83 |
| 0.60 | 1.71 |
| 0.80 | 1.58 |
| 1.00 | 1.45 |

(3) Notched circular hole with $\beta = 45^\circ$ (small edge crack in a sheet subjected to uniaxial tension):

$$\Delta K = 1.12 \Delta \sigma_t \sqrt{\pi a} \quad (4)$$

where

$$\sigma_t = \sigma_o \text{ for } \beta = 45^\circ$$

Although three different notch geometries with varying size and tip radius were tested, the results indicated that $\Delta K/K_a$ is the main governing parameter for fatigue-crack initiation from a blunt flaw. The results were consistent for all specimens tested, and especially for flaws with a length-to-tip-radius ratio, a/ρ , greater than 5.

The experimental results shown in Figure 4 are for cycles to crack initiation ranging from unity to greater than 2×10^6 . The results consisted of both plastic and elastic deformation at the flaw tips. Plastic deformation was assumed to occur when the maximum stress was greater than the tensile yield stress and elastic deformation when the maximum stress was less than the tensile yield stress.

To determine whether the deformation was elastic or plastic, two methods of analysis were used: one was to use the following solution (Reference 7) for the maximum stress at the boundary of an elliptical hole in a large plate subjected to uniaxial tension:

$$\sigma_t = \sigma_o + 2\sigma_o \sqrt{\frac{a}{\rho}} \quad (5)$$

Rewriting Equation 5 to be in terms of the stress-intensity factor gives the following equation which can be used for determining whether the maximum stresses are greater or less than the tensile yield stress:

$$\sigma_t = \sigma_o + \frac{2K}{\sqrt{\pi\rho}} \quad (6)$$

Another useful approach which gives nearly the same results in determining type of deformation is to note that elastic deformation occurs when ρ/w is greater than 8.0 for plane stress, and 6.5 for plane strain. For these values,

Table II shows the yield-zone boundary to coincide with the notch tip boundary, or, in other words, the notch tip is at the onset of yielding.

For the specimens that had no yielding at the notch tip, the maximum stresses were calculated by using Equation 6. Comparisons were made between the data in Table I and the fatigue data in References 12 and 13. One interesting result was that the endurance limit stress for the flawed specimens was approximately 60,000 psi at flaw tip. This is double the endurance limit stress for smooth or unnotched specimens of the same material. The results are in agreement then with current fatigue data, which shows that very sharp notches have less effect on fatigue strength than might be expected in view of their high theoretical stress-concentration factors.

For the data shown in Figure 4 and listed in Table I, crack initiation was defined as the load cycle when a .010-inch crack was first observed. A question arises, however, as to what percentage of the cyclic behavior was nucleation of a fatigue crack and what percentage was propagation to the "engineering size" crack. An estimate of the percentage can be obtained by using the crack growth theory presented in Reference 1. The theory states that crack growth per load cycle is given by the equation

$$\frac{da}{dN} = \frac{C(\Delta K)^n}{(1-R)K_c - \Delta K} \quad (7)$$

For the material tested, Figure 3 indicates that K_c equals 50,000 psi $\sqrt{\text{in}}$, and from Reference 1, n equals 3.0 and C equals 5×10^{-13} . We assigned da the value .010 inch, then calculated dN for different values of $\Delta K/K_c$. The results are shown by the dashed curve in Figure 4. The curve indicates that, theoretically, a large percentage of the behavior was crack propagation and only a small percentage was nucleation. In fact, the theoretical crack propagation curve is a very good representation of the lower boundary of the data. For flaws where the ratio a/ρ is greater than 5, a satisfactory approach for predicting cycles to initiation of an "engineering size" crack is to use crack propagation theory in which it is assumed that crack growth begins with the first load cycle.

To determine whether or not similar results occur for a different material, Manson's data (Reference 8) for 2014-T6 aluminum alloy was put in the form of $\Delta K/K_a$ versus N_i and plotted in Figure 5. For this data, N_i was for the initiation of an average crack length of .0025 inch. The results are very similar to the 7075-T6 aluminum alloy results, and the crack propagation analysis shows that for this defined crack length, most of the behavior was also crack propagation. The analysis was made using K_c equal to 30,000 psi $\sqrt{\text{in}}$ (Reference 9); C equal to 3×10^{-13} , and $n = 3.0$, both of which were obtained from the data in References 10 and 11.

Finally, the calculations resulting from $\Delta K/K_a$ versus N_i from Figure 4 were used in an analysis to determine the size limit of a flaw which would not have an effect on the fatigue life. The results of the analysis are shown in Figure 6. A comparison of the crack initiation curves with unnotched S-N fatigue curves shows that a flaw size of approximately .005 inch would be the limiting size before fatigue life in 7075-T6 aluminum sheet material would be affected. Smaller flaws than .005 inch could be neglected.

REFERENCES

1. R. G. Forman, V. E. Kearney, and R. M. Engle, "Numerical Analysis of Crack Propagation in Cyclic-Loaded Structures," J. of Basic Engineering, Trans. ASME, Series D, Vol. 89, September 1967, pp. 459-464.
2. C. M. Hudson and J. T. Scardina, "Effect of Stress Ratio on Fatigue-Crack Growth in 7075-T6 Aluminum-Alloy Sheet," Presented at the National Symposium on Fracture Mechanics, Bethlehem, Pennsylvania, June 19-21, 1967.
3. P. C. Paris and F. Erdogan, "A Critical Analysis of Crack Propagation Laws," J. of Basic Engineering, Trans. ASME, Series D, Vol. 85, 1963, pp. 528-534.
4. J. Schijve, "Significance of Fatigue Cracks in Micro-Range and Macro-Range," Fatigue Crack Propagation, ASTM STP 415, 1967, pp. 415-459.
5. J. H. Mulherin, D. F. Armiento, and H. Markus, "The Relationship Between Fracture Toughness and Stress Concentration Factors for Several High-Strength Aluminum Alloys," J. of Basic Engineering, Trans. ASME, Series D, Vol. 86, 1964, pp. 709-717.
6. P. C. Paris and G. C. Sih, "Stress Analysis of Cracks," Fracture Toughness Testing and Its Applications, ASTM STP 381.
7. S. Timoshenko and J. N. Goodier, Theory of Elasticity, McGraw-Hill Book Company, Inc., New York, 1951.
8. S. S. Manson, "Fatigue: A Complex Subject - Some Simple Approximations," Experimental Mechanics, July 1965, pp. 193-226.
9. T. W. Orange, "Fracture Toughness of Wide 2014-T6 Aluminum Sheet at -320°F," NASA TN D-4017, June 1967.
10. D. R. Donaldson and W. E. Anderson, "Crack Propagation Behavior of Some Airframe Materials," Proceedings of Crack Propagation Symposium, College of Aeronautics, Cranfield, England, Vol. 2, September 1961, pp. 375-441.
11. W. D. Nelson, Residual Crack Strength and Fatigue Crack Propagation Data for Four Aluminum Alloys, Engineering Technical Report No. 32145, Douglas Aircraft Division, Douglas Aircraft Company, September 1, 1965.
12. C. R. Smith, A Method for Estimating the Fatigue Life of 7075-T6 Aluminum Alloy Aircraft Structures, Aeronautical Structures Laboratory Report No. NAEC-ASL-1096, U.S. Naval Air Engineering Center, December 1965.
13. B. J. Lazon and A. A. Blatherwick, Fatigue Properties of Aluminum Alloys at Various Direct Stress Ratios, Part 1. Rolled Alloys, WADC TR 52-307, Part 1, September 1953.

REFERENCES (Continued)

14. W. H. Munse, W. H. Bruckner, A. J. Hartman, J. B. Radzinski, R. W. Hinton, and J. L. Mooney, Studies of the Fatigue Behavior of Butt-Welded Joints in HY-80 and HY-100 Steels, A Report of an Investigation Conducted by the Civil Engineering Department, U. of Illinois, in cooperation with the Bureau of Ships, U.S. Navy, November 1964 (AD No. 452191).
15. M. Creager, The Elastic Stress Field Near the Tip of a Blunt Crack, Thesis for the Degree of Master of Science, Lehigh University, 1966.

APPENDIX

THE YIELD ZONE AT THE TIP OF A BLUNT CRACK

The elastic stresses in an infinite plate which contains a blunt crack and is subjected to uniaxial tension perpendicular to the crack direction can be found by the following relations obtained from Reference 15:

$$\sigma_x = \frac{K}{(2\pi r)^{1/2}} \cos \frac{\theta}{2} \left[1 - \sin \frac{\theta}{2} \sin \frac{3\theta}{2} \right] - \frac{K}{(2\pi r)^{1/2}} \frac{\rho}{2r} \cos \frac{3}{2}\theta \quad (8)$$

$$\sigma_y = \frac{K}{(2\pi r)^{1/2}} \cos \frac{\theta}{2} \left[1 + \sin \frac{\theta}{2} \sin \frac{3\theta}{2} \right] + \frac{K}{(2\pi r)^{1/2}} \frac{\rho}{2r} \cos \frac{3}{2}\theta \quad (9)$$

$$\tau_{xy} = \frac{K}{(2\pi r)^{1/2}} \sin \frac{\theta}{2} \cos \frac{\theta}{2} \cos \frac{3\theta}{2} - \frac{K}{(2\pi r)^{1/2}} \frac{\rho}{2r} \sin \frac{3}{2}\theta \quad (10)$$

If the yield-zone size is small compared to the region in which the elastic stresses given by the above equations are valid, then outside the yield zone these stresses are still a reasonable approximation. If they are accurate up to the boundary of the yield zone, an estimate of the size and shape of the yield zone may be obtained.

By substituting the stresses, as defined in Equations 8, 9, and 10, into the "Distortion Energy" yield criterion that is,

$$\frac{1}{2} (S_x^2 + S_y^2 + S_z^2) + (\tau_{xy}^2 + \tau_{xz}^2 + \tau_{yz}^2) = \frac{Y^2}{3} \quad (11)$$

where

$$S = \frac{\sigma_x + \sigma_y + \sigma_z}{3}$$

and

$$S_x = \sigma_x - S$$

$$S_y = \sigma_y - S$$

$$S_z = \sigma_z - S$$

the following equation is obtained for the radius vector, r , of the locus of points on the boundary of the yield zone:

$$r^3 - wF(\theta)r^2 - \frac{3}{4}w\rho^2 = 0 \quad (12)$$

In Equation 12

$$w = \frac{1}{2\pi} \left(\frac{K}{Y} \right)^2$$

and is the yield zone width for $\rho = 0$; the expression for plane stress is

$$F(\theta) = \cos^2 \frac{\theta}{2} \left[1 + 3 \sin^2 \frac{\theta}{2} \right]$$

and for plane strain is

$$F(\theta) = \cos^2 \frac{\theta}{2} \left[(1 - 2\mu)^2 + 3 \sin^2 \frac{\theta}{2} \right]$$

Equation 12 is an algebraic cubic equation which has one real root. The root has the following form when written in terms of r/w , the relative yield-zone size:

$$\begin{aligned} \frac{r}{w} = & \frac{F(\theta)}{3} + \left[\left(\frac{F(\theta)}{3} \right)^3 + 2Q + 2\sqrt{Q\left(\frac{F(\theta)}{3}\right)^3 + Q^2} \right]^{1/3} \\ & + \left[\left(\frac{F(\theta)}{3} \right)^3 + 2Q - 2\sqrt{Q\left(\frac{F(\theta)}{3}\right)^3 + Q^2} \right]^{1/3} \end{aligned} \quad (13)$$

where

$$Q = \frac{3}{16} \left(\frac{\rho}{w} \right)^2$$

Equation 13 indicates that r/w is a function only of the relative notch root radius, ρ/w . For comparison, the size and shape of the relative yield zone for a blunt notch and a sharp notch are shown in Figure 7.

By setting $r = r_p$ for $\theta = 0$, the width of the yield-zone boundary can be determined for different notch root radii. The widths were calculated for important ranges of ρ/w , and the results are given in Table II. The comparison of r_p/w versus ρ/w for both plane stress and plane strain is shown in Figure 2.

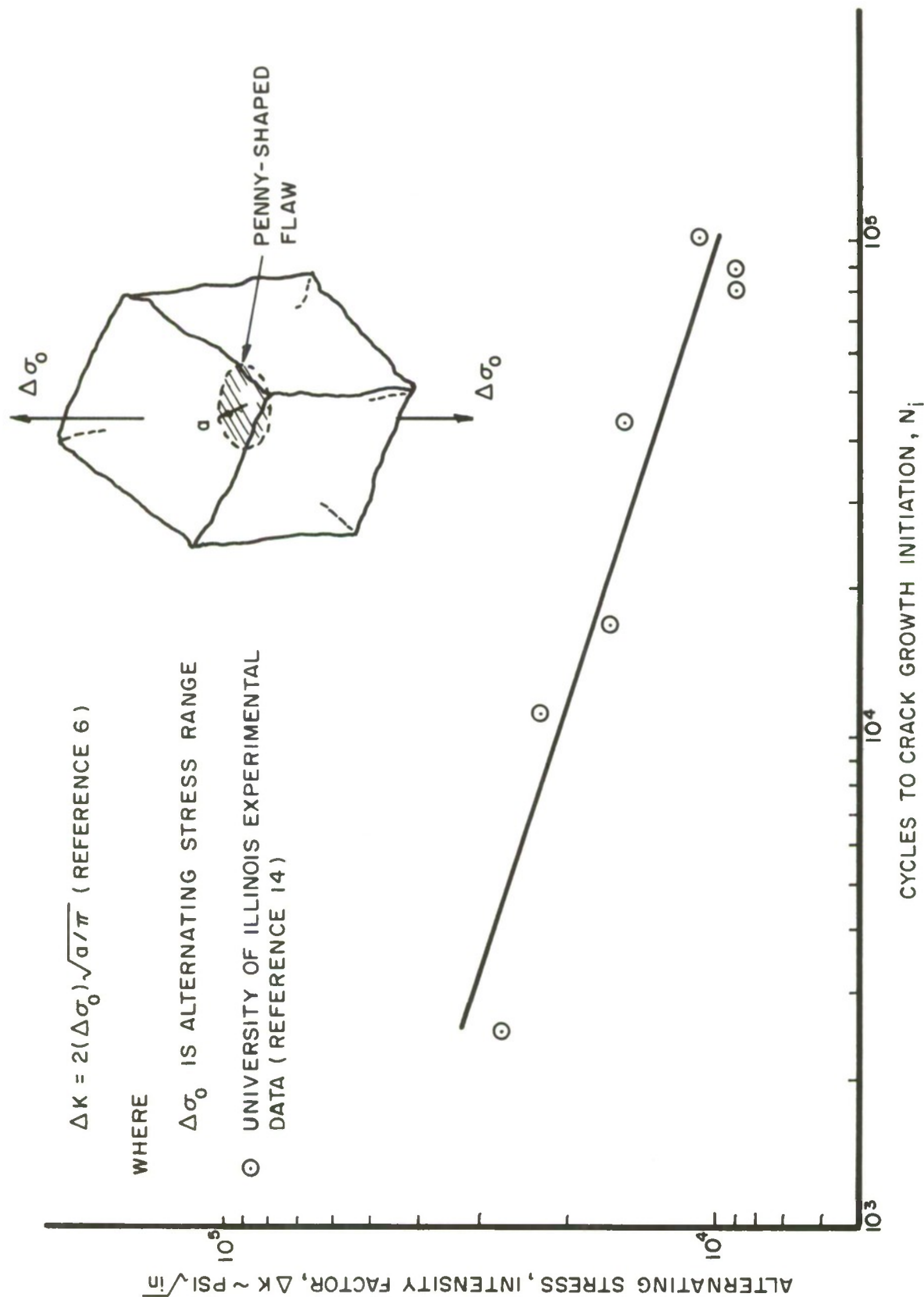


Figure 1. Variation in K with N_i for Flaws in Butt-Welded 3/4-Inch-Thick HY-80 Steel Strips

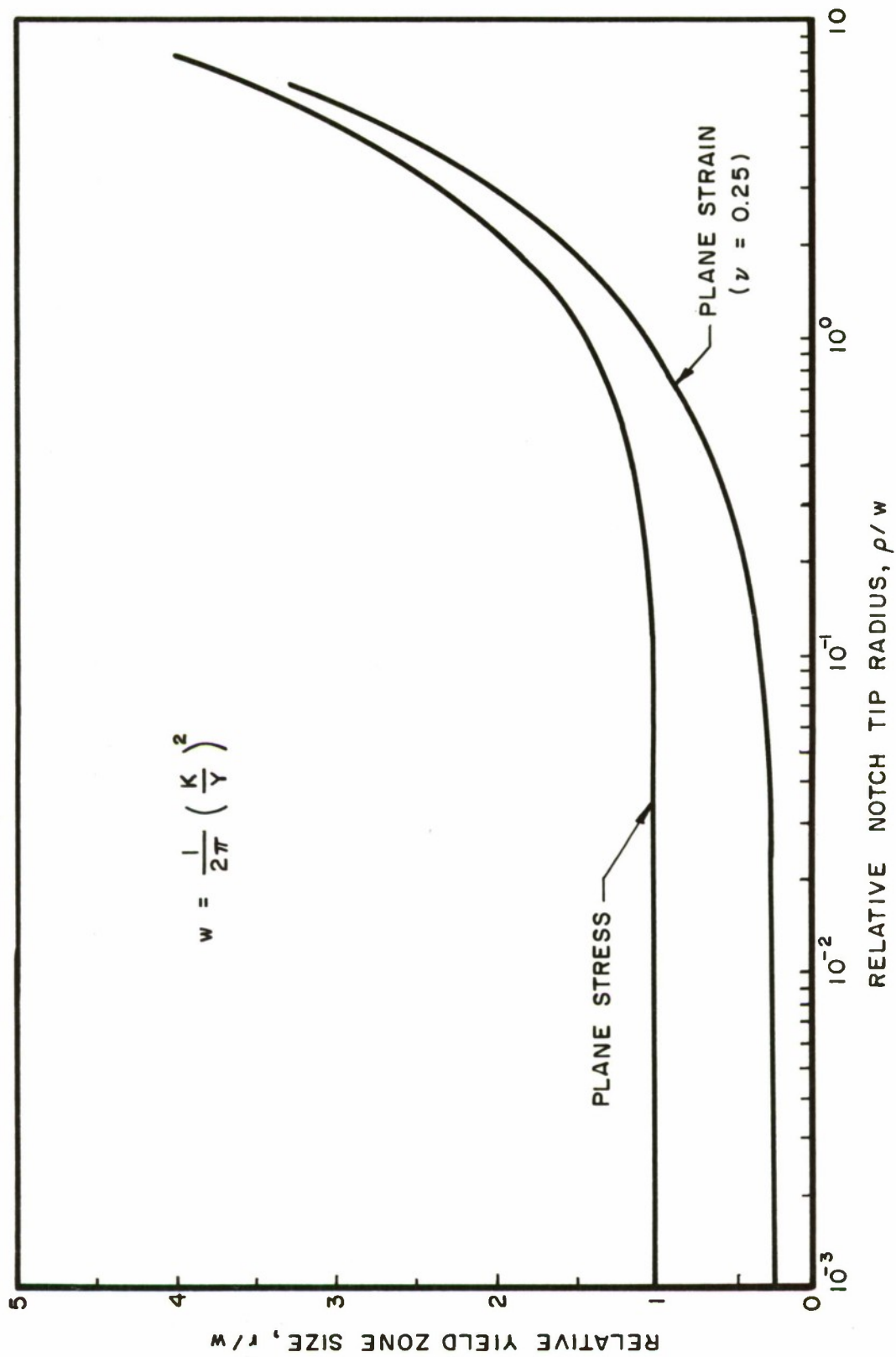


Figure 2. Variation in Yield-Zone Size with Notch Tip Radius

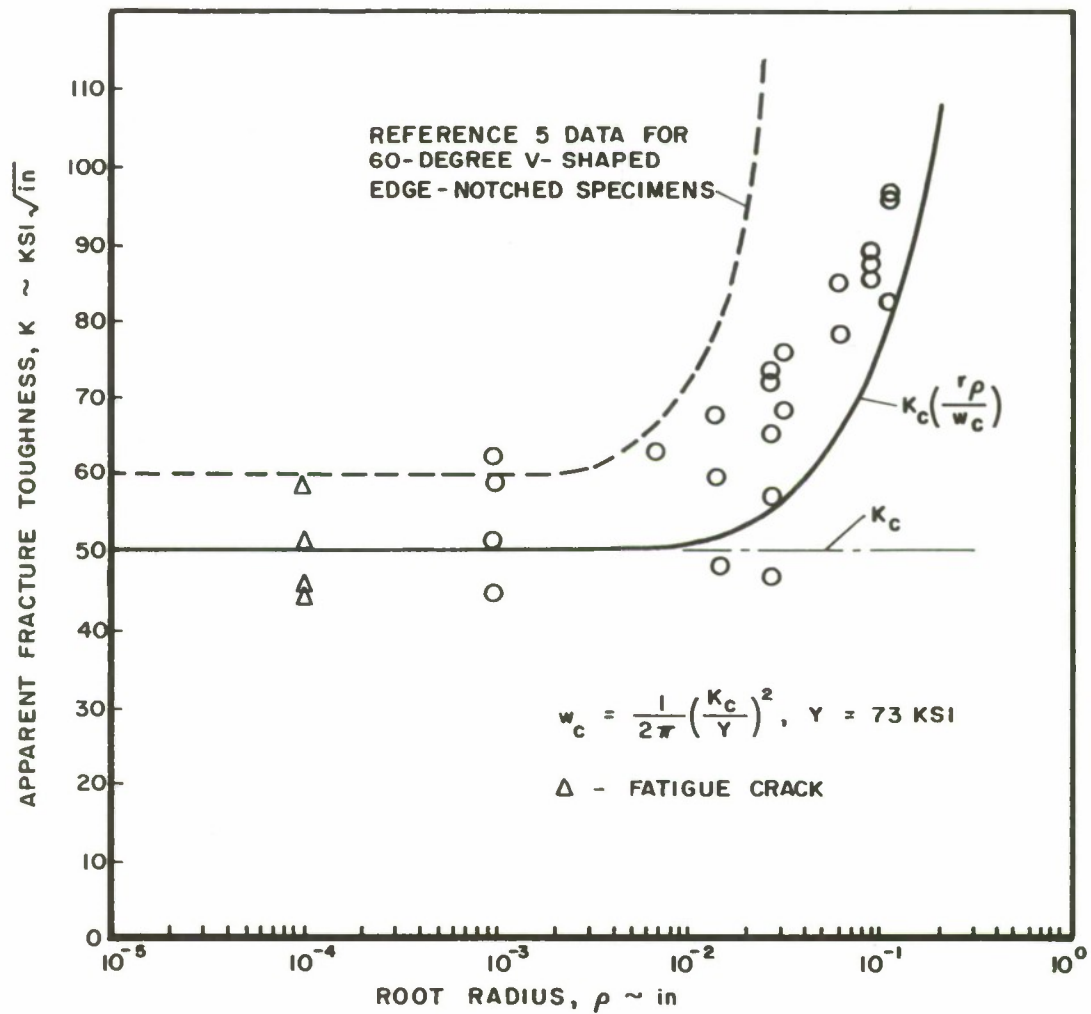


Figure 3. Variation of Apparent Fracture Toughness with Root Radius for Centrally Notched 7075-T6 Aluminum Plates

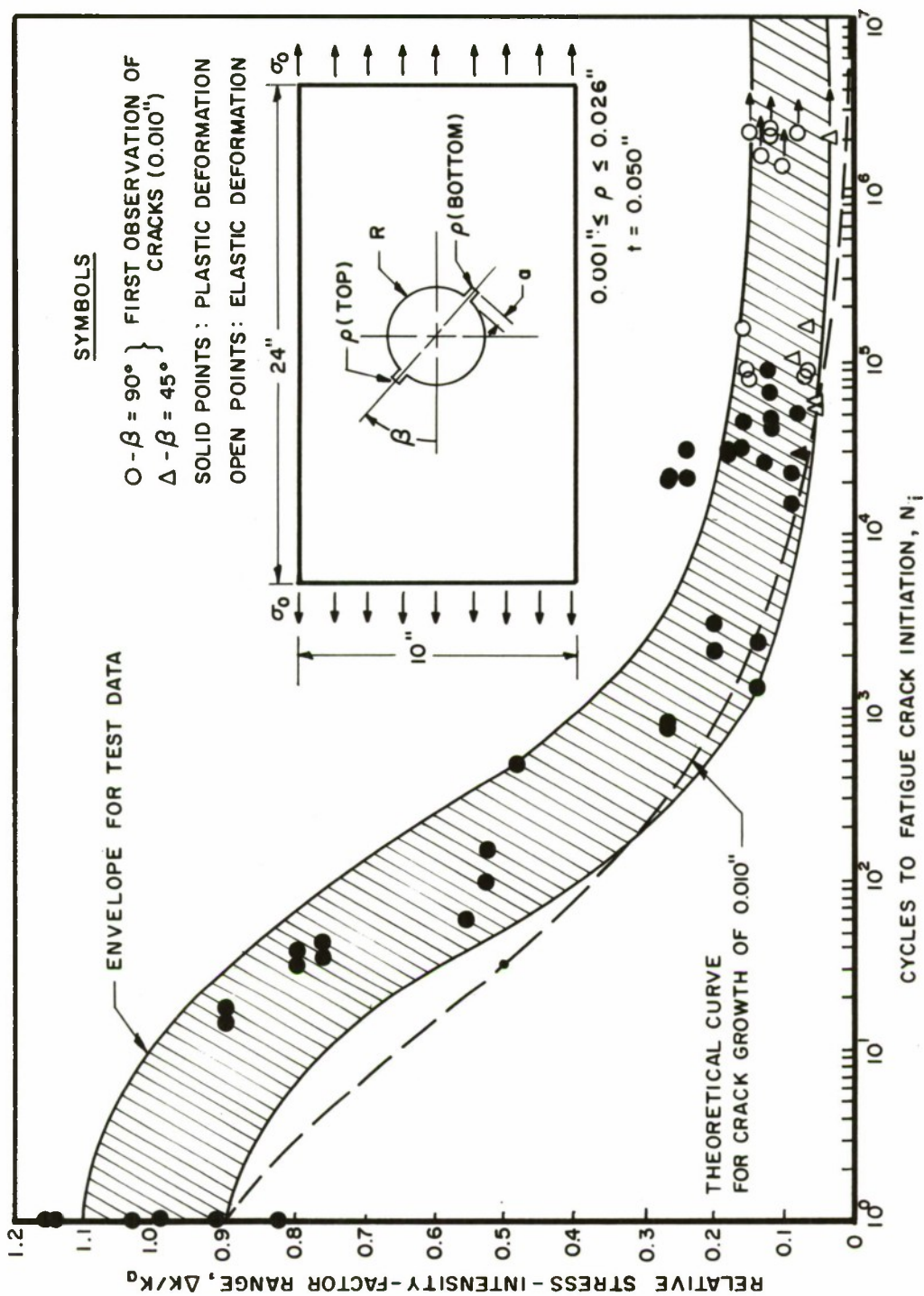


Figure 4. Comparison of Theoretical Crack Growth of .010-Inch with First Observation of .010-Inch Fatigue Cracks in Notched Sheets of 7075-T6 Aluminum

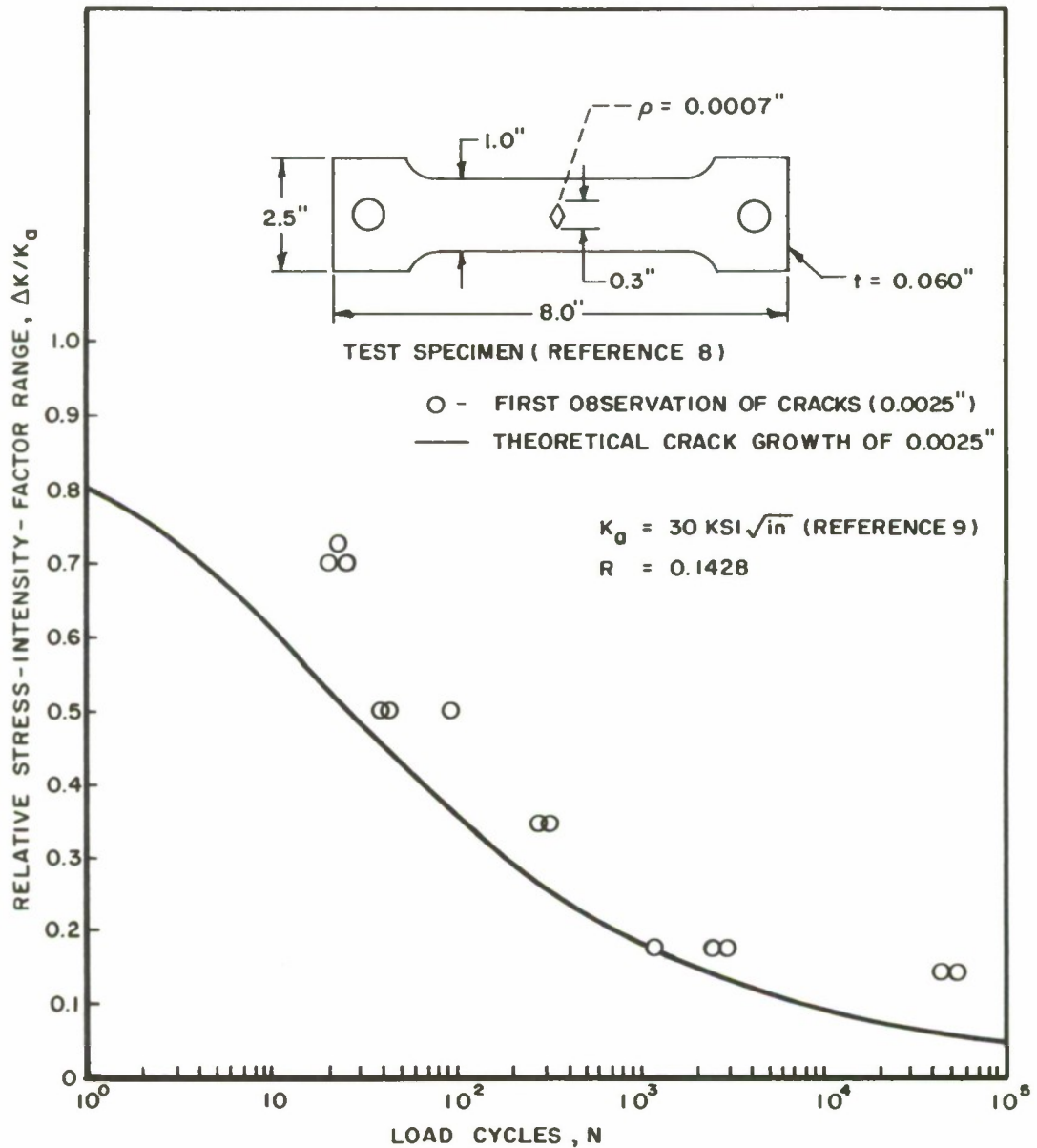


Figure 5. Comparison of Theoretical Crack Growth of .0025-Inch with First Observation of .0025-Inch Fatigue Cracks in Notched Sheets of 2014-T6 Aluminum

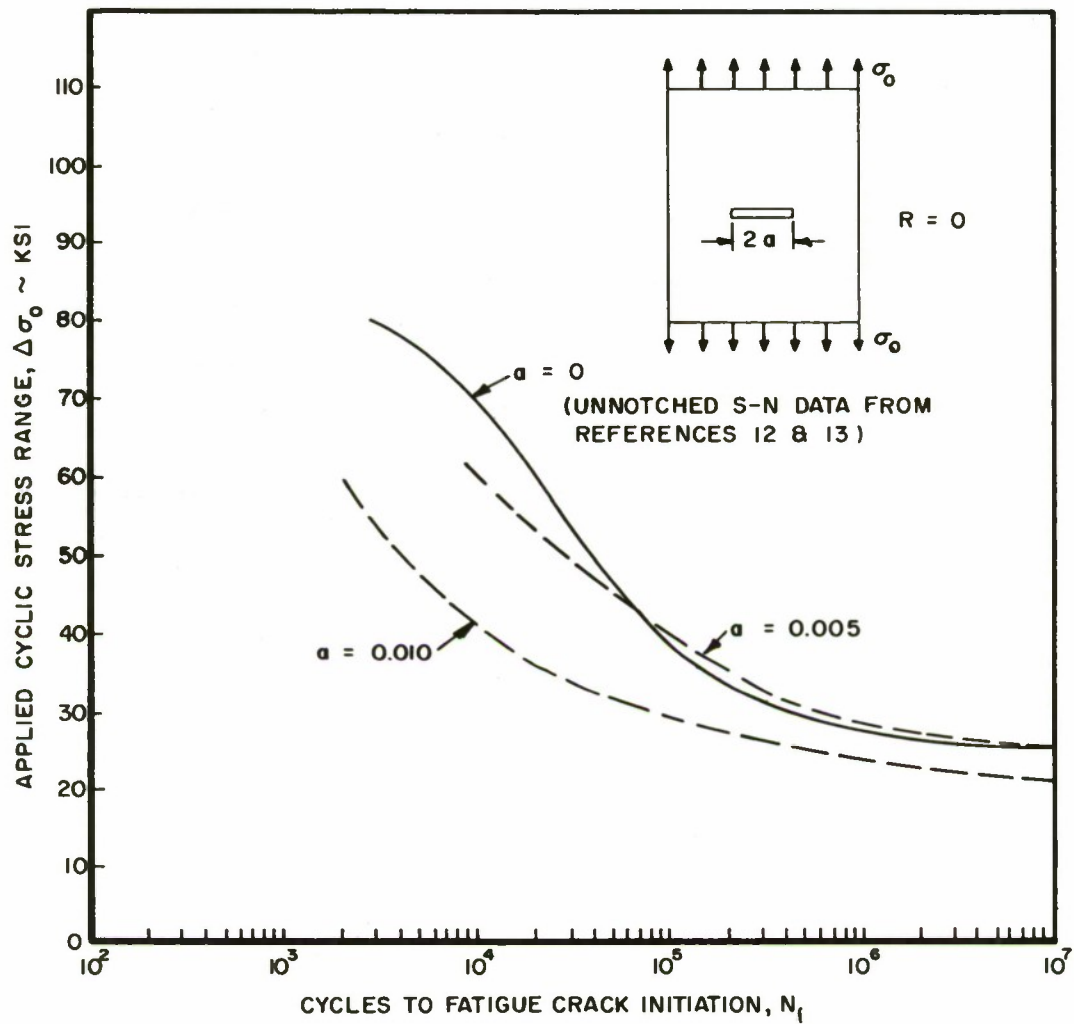


Figure 6. Comparison of Applied Cyclic Stress Range with Cycles to Fatigue Crack Initiation from Blunt Flaws in 7075-T6 Aluminum Plates

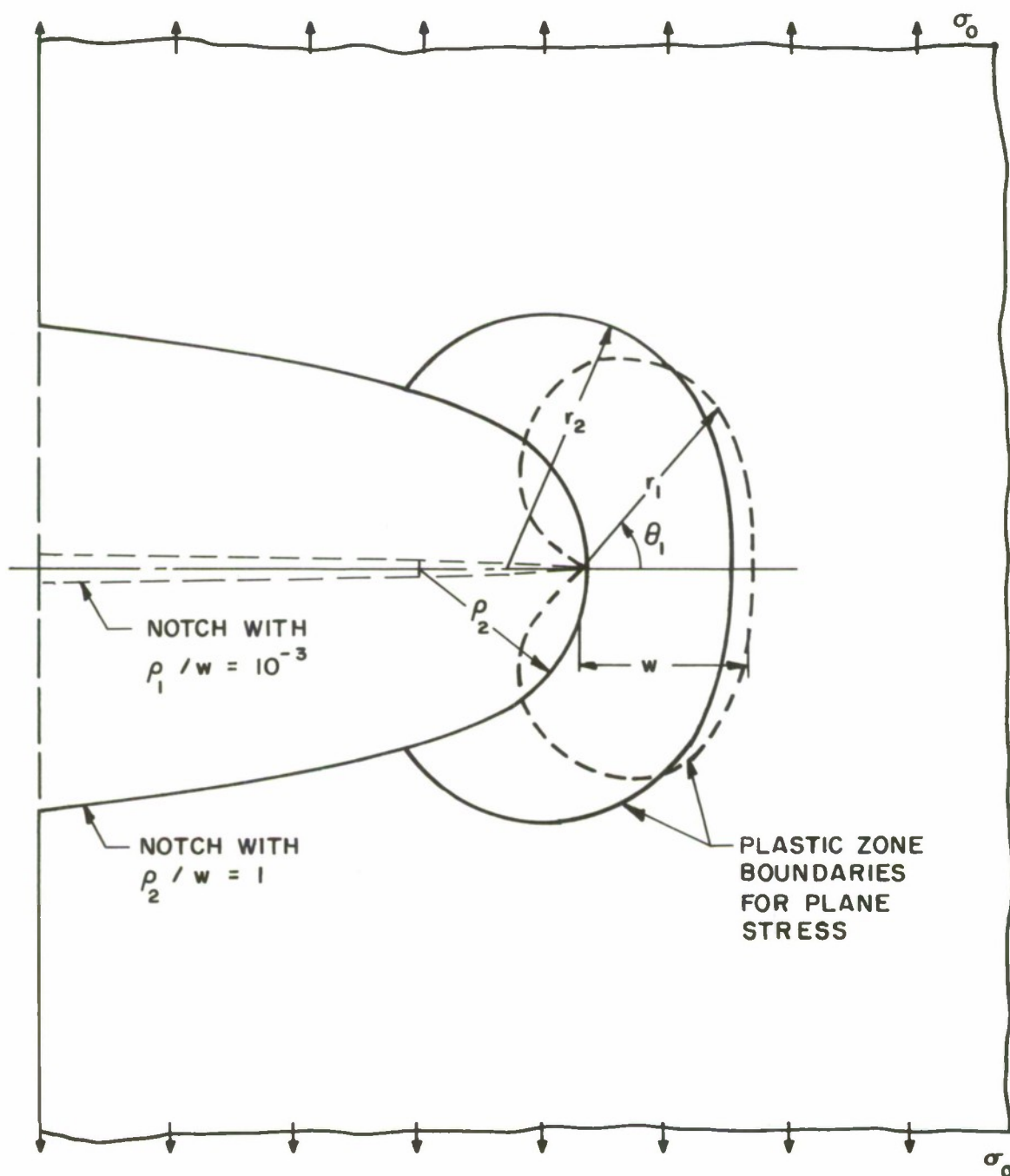


Figure 7. Geometry of Plastic Zone Boundaries at the Tip of Sharp and Blunt Elliptic Notches in a Plate Subjected to Uniaxial Tension

TABLE I

TEST DATA FOR INITIATION OF .010-INCH CRACKS IN .050-INCH-THICK 7075-T6
ALUMINUM SHEET SPECIMENS FATIGUE CYCLED AT R = 0

| Specimen Number | R (in) | α (in) | β (degrees) | ρ (in) | $\Delta\sigma_0$ (psi) | N _i (cycles)**** | |
|--------------------|-----------|------------------|----------------------|----------------|---------------------------|-----------------------------|--------------------------|
| | | | | | | Top ρ | Bottom ρ |
| 1 | 1.0 | 0.10 | 90 | .001 | 33,720 | 1 | 1 |
| 2 | 1.0 | 0.10 | 90 | .001 | 18,200 | 60 | 60 |
| 3 | 1.0 | 0.10 | 90 | .001 | 4,550 | 1,351 | 2,539 |
| 4 | 1.0 | 0.10 | 90 | .026 | 31,000 | 1 | 1 |
| 5 | 1.0 | 0.10 | 90 | .026 | 9,100 | 30,000 | 21,100 |
| 6 | 1.0 | 0.10 | 90 | .026 | 18,200 | 470 | 470 |
| 7 | 1.0 | 0.10 | 90 | .026 | 4,550 | 2 x 10 ⁶ * | 2 x 10 ⁶ * |
| 8 | 1.0 | 0.10 | 90 | .013 | 31,600 | 1 | 1 |
| 9 | 1.0 | 0.10 | 90 | .013 | 18,200 | 150 | 100 |
| 10 | 1.0 | 0.10 | 90 | .013 | 9,100 | 750 | 800 |
| 11 | 1.0 | 0.10 | 90 | .026 | 4,550 | 2 x 10 ⁶ * | 2 x 10 ⁶ * |
| 12 | 1.0 | 0.10 | 90 | .013 | 4,550 | 26,372 | 26,372 |
| 13 | 1.0 | 0.10 | 90 | .026 | 6,824 | 29,022 | 32,000 |
| 14 | 1.0 | 0.10 | 90 | .026 | 6,000 | 81,000 | 81,000 |
| 15 | 1.0 | 0.10 | 90 | .007 | 2,600 | 2.13 x 10 ⁶ * | 2.13 x 10 ⁶ * |
| 16 | 1.0 | 0.10 | 90 | .007 | 6,500 | 2,100 | 3,000 |
| 17 | 1.0 | 0.10 | 90 | .007 | 3,900 | 48,600 | 63,600 |
| 18 | 1.0 | 0.10 | 90 | .007 | 5,200 | 31,500 | 45,000 |
| 19 | 0 | 1.15 | 90 | .026 | 30,000 | 1 | 1 |
| 20 | 0 | 1.15 | 90 | .001 | 30,590 | 1 | 1 |
| 21 | 0 | 1.15 | 90 | .001 | 30,000 | 1 | 1 |
| 22 | 0 | 1.15 | 90 | .026 | 4,800 | 86,400 | 157,430 |
| 23 | 1.0 | 0.025 | 90 | .007 | 7,440 | 21,318 | 21,628 |
| 24 | 1.0 | 0.025 | 90 | .007 | 4,300 | 2 x 10 ⁶ * | 2 x 10 ⁶ * |
| 25 | 1.0 | 0.025 | 90 | .004 | 3,750 | 1.6 x 10 ⁶ * | 1.6 x 10 ⁶ * |
| 26 | 1.0 | 0.025 | 90 | .002 | 2,810 | 1.4 x 10 ⁶ * | 1.4 x 10 ⁶ * |
| 27 | 0 | 1.15 | 90 | .007 | 33,170 | 1 | 1 |
| 28 | 1.0 | 0.033 | 45 | .007 | 10,000 | 137,883 | ** |
| 29 | 0 | 1.15 | 90 | .013 | 35,742 | 1 | 1 |
| 30 | 1.0 | 0.030 | 45 | .007 | 13,230 | 101,943 | ** |
| 31 | 0 | 1.15 | 90 | .026 | 38,318 | 1 | 1 |
| 32 | 1.0 | 0.025 | 45 | .002 | 14,000 | 29,862 | 49,801 |
| 33 | 1.0 | 0.028 | 45 | .001 | 5,600 | 2 x 10 ⁶ * | 2 x 10 ⁶ * |
| 34 | 0 | 1.15 | 90 | .031 | 40,000 | 1 | 1 |
| 35 | 1.0 | 0.010 | 45 | .001 | 15,810 | 53,630 | 56,692 |
| 36 | 1.0 | 0.010 | 90 | .002 | 6,000 | 88,698 | 75,173 |
| 37 | 1.0 | 0.010 | 90 | .001 | 8,000 | 15,241 | 22,498 |
| 38 | 0 | 1.15 | 90 | .007 | 20,000 | 36 | 42 |
| 39 | 0 | 0.50 | 90 | .007 | 4,730 | 89,230 | 41,860 |
| 40 | 0 | 0.50 | 90 | .007 | 36,000 | 15 | 18 |
| 41 | 0 | 0.50 | 90 | .007 | 32,000 | 34 | 36 |
| 42 | 0 | 1.15 | 90 | .125 | 50,550 | 1 | 1 |
| 43 | 0 | 1.15 | 90 | .093 | 45,720 | 1 | 1 |
| 44 | 0 | 1.15 | 90 | .125 | 50,716 | 1 | 1 |
| 45 | 0 | 1.15 | 90 | .031 | 36,000 | 1 | 1 |
| 46 | 0 | 1.15 | 90 | .062 | 44,760 | 1 | 1 |
| 47 | 0 | 1.15 | 90 | .062 | 41,200 | 1 | 1 |
| 48 | 0 | 1.15 | 90 | .093 | 46,700 | 1 | 1 |
| 49 | 0 | 1.15 | 90 | .093 | 45,080 | 1 | 1 |
| 50 | 0 | 1.15 | 90 | .125 | 43,400 | 1 | 1 |
| 16Repeat | 1.0 | 0.110 | 90 | *** | 28,830 | 1 | 1 |
| 18Repeat | 1.0 | 0.270 | 90 | *** | 25,960 | 1 | 1 |
| 22Repeat | 0 | 1.40 | 90 | *** | 24,480 | 1 | 1 |
| 38Repeat | 0 | 1.74 | 90 | *** | 19,160 | 1 | 1 |

* No cracks

** Not measured

*** Fatigue Crack

**** See Figure 4 for Description of Top ρ and Bottom ρ

TABLE II
THEORETICAL VALUES OF PLASTIC ZONE SIZE

| ρ/w | r_p/w | |
|----------|--------------|---------------|
| | PLANE STRESS | PLANE STRAIN* |
| .0001 | 1.0000 | .2500 |
| .001 | 1.0000 | .2500 |
| .01 | 1.0000 | .2512 |
| .02 | 1.0002 | .2546 |
| .04 | 1.0011 | .2670 |
| .06 | 1.0027 | .2836 |
| .08 | 1.0048 | .3025 |
| .10 | 1.0073 | .3222 |
| .12 | 1.0105 | .3422 |
| .14 | 1.0143 | .3622 |
| .16 | 1.0185 | .3816 |
| .18 | 1.0231 | .4010 |
| .20 | 1.0283 | .4200 |
| .30 | 1.0600 | .5098 |
| .40 | 1.0992 | .5920 |
| .50 | 1.1434 | .6690 |
| .60 | 1.1905 | .7413 |
| .70 | 1.2392 | .8101 |
| .80 | 1.2889 | .8757 |
| .90 | 1.3388 | .9390 |
| 1.0 | 1.3888 | 1.0000 |
| 1.2 | 1.4883 | 1.116 |
| 1.4 | 1.584 | 1.226 |
| 1.6 | 1.679 | 1.332 |
| 1.8 | 1.772 | 1.432 |
| 2.0 | 1.8627 | 1.530 |
| 2.5 | 2.081 | 1.761 |
| 3.0 | 2.2879 | 1.977 |
| 3.5 | 2.486 | 2.181 |
| 4.0 | 2.6766 | 2.375 |
| 4.5 | 2.858 | 2.563 |
| 5.0 | 2.9975 | 2.742 |
| 5.5 | 3.206 | 2.915 |
| 6.0 | 3.3400 | 3.085 |
| 6.5 | 3.5038 | 3.250 |
| 7.0 | 3.6626 | ** |
| 7.5 | 3.8195 | ** |
| 8.0 | 3.9724 | ** |

* = 0.25

** No Plastic Deformation

| DOCUMENT CONTROL DATA - R&D | | |
|---|---|------------------------------------|
| (Security classification of title, body of abstract and indexing annotation must be entered when the overall report is classified) | | |
| 1. ORIGINATING ACTIVITY (Corporate author) Air Force Flight Dynamics Laboratory Wright-Patterson Air Force Base, Ohio | | 2a. REPORT SECURITY CLASSIFICATION |
| | | 2b. GROUP |
| 3. REPORT TITLE STUDY OF FATIGUE CRACK INITIATION FROM FLAWS USING FRACTURE MECHANICS THEORY | | |
| 4. DESCRIPTIVE NOTES (Type of report and inclusive dates) | | |
| 5. AUTHOR(S) (Last name, first name, initial) Forman, R. G. | | |
| 6. REPORT DATE September 1968 | 7a. TOTAL NO. OF PAGES 38 | 7b. NO. OF REFS 15 |
| 8a. CONTRACT OR GRANT NO. | 9a. ORIGINATOR'S REPORT NUMBER(S) AFFDL-TR-68-100 | |
| b. PROJECT NO. 1467 | | |
| c. Task 146704 | 9b. OTHER REPORT NO(S) (Any other numbers that may be assigned this report) | |
| d. | | |
| 10. AVAILABILITY/LIMITATION NOTICES This document is subject to special export controls and each transmittal to foreign governments or foreign nationals may be made only with prior approval of the Air Force Flight Dynamics Laboratory (FDTR), Wright-Patterson AFB, Ohio 45433. In DDC. | | |
| 11. SUPPLEMENTARY NOTES | 12. SPONSORING MILITARY ACTIVITY Air Force Flight Dynamics Laboratory Wright-Patterson Air Force Base, Ohio | |
| 13. ABSTRACT This report presents theoretical and experimental results on fatigue crack initiation from flaws in cyclic loaded structures. The results indicated that the fracture mechanics stress-intensity-factor range, ΔK , is the governing parameter for inducing fatigue crack initiation from a flaw. Theoretical crack growth analysis indicated that when initiating an "engineering size" fatigue crack from a flaw, most of the cyclic behavior was crack growth and only a small part was nucleation. This abstract is subject to special export controls and each transmittal to foreign governments or foreign nationals may be made only with prior approval of the Air Force Flight Dynamics Laboratory (FDTR), Wright-Patterson AFB, Ohio. | | |

| | | | | | | |
|--|--------|----|--------|----|--------|----|
| 14. KEY WORDS | LINK A | | LINK B | | LINK C | |
| | ROLE | WT | ROLE | WT | ROLE | WT |
| Fatigue Crack Propagation Fracture Mechanics Crack Initiation Aluminum | | | | | | |

INSTRUCTIONS

1. ORIGINATING ACTIVITY: Enter the name and address of the contractor, subcontractor, grantee, Department of Defense activity or other organization (*corporate author*) issuing the report.

2a. REPORT SECURITY CLASSIFICATION: Enter the overall security classification of the report. Indicate whether "Restricted Data" is included. Marking is to be in accordance with appropriate security regulations.

2b. GROUP: Automatic downgrading is specified in DoD Directive 5200.10 and Armed Forces Industrial Manual. Enter the group number. Also, when applicable, show that optional markings have been used for Group 3 and Group 4 as authorized.

3. REPORT TITLE: Enter the complete report title in all capital letters. Titles in all cases should be unclassified. If a meaningful title cannot be selected without classification, show title classification in all capitals in parenthesis immediately following the title.

4. DESCRIPTIVE NOTES: If appropriate, enter the type of report, e.g., interim, progress, summary, annual, or final. Give the inclusive dates when a specific reporting period is covered.

5. AUTHOR(S): Enter the name(s) of author(s) as shown on or in the report. Enter last name, first name, middle initial. If military, show rank and branch of service. The name of the principal author is an absolute minimum requirement.

6. REPORT DATE: Enter the date of the report as day, month, year, or month, year. If more than one date appears on the report, use date of publication.

7a. TOTAL NUMBER OF PAGES: The total page count should follow normal pagination procedures, i.e., enter the number of pages containing information.

7b. NUMBER OF REFERENCES: Enter the total number of references cited in the report.

8a. CONTRACT OR GRANT NUMBER: If appropriate, enter the applicable number of the contract or grant under which the report was written.

8b, 8c, & 8d. PROJECT NUMBER: Enter the appropriate military department identification, such as project number, subproject number, system numbers, task number, etc.

9a. ORIGINATOR'S REPORT NUMBER(S): Enter the official report number by which the document will be identified and controlled by the originating activity. This number must be unique to this report.

9b. OTHER REPORT NUMBER(S): If the report has been assigned any other report numbers (*either by the originator or by the sponsor*), also enter this number(s).

10. AVAILABILITY/LIMITATION NOTICES: Enter any limitations on further dissemination of the report, other than those

imposed by security classification, using standard statements such as:

- (1) "Qualified requesters may obtain copies of this report from DDC."
- (2) "Foreign announcement and dissemination of this report by DDC is not authorized."
- (3) "U. S. Government agencies may obtain copies of this report directly from DDC. Other qualified DDC users shall request through _____."
- (4) "U. S. military agencies may obtain copies of this report directly from DDC. Other qualified users shall request through _____."
- (5) "All distribution of this report is controlled. Qualified DDC users shall request through _____."

If the report has been furnished to the Office of Technical Services, Department of Commerce, for sale to the public, indicate this fact and enter the price, if known.

11. SUPPLEMENTARY NOTES: Use for additional explanatory notes.

12. SPONSORING MILITARY ACTIVITY: Enter the name of the departmental project office or laboratory sponsoring (paying for) the research and development. Include address.

13. ABSTRACT: Enter an abstract giving a brief and factual summary of the document indicative of the report, even though it may also appear elsewhere in the body of the technical report. If additional space is required, a continuation sheet shall be attached.

It is highly desirable that the abstract of classified reports be unclassified. Each paragraph of the abstract shall end with an indication of the military security classification of the information in the paragraph, represented as (TS), (S), (C), or (U).

There is no limitation on the length of the abstract. However, the suggested length is from 150 to 225 words.

14. KEY WORDS: Key words are technically meaningful terms or short phrases that characterize a report and may be used as index entries for cataloging the report. Key words must be selected so that no security classification is required. Identifiers, such as equipment model designation, trade name, military project code name, geographic location, may be used as key words but will be followed by an indication of technical context. The assignment of links, rules, and weights is optional.